Editors' Suggestion Featured in Physics

Free-Electron–Bound-Electron Resonant Interaction

Avraham Gover [1,*] and Amnon Yariv [2]
[1] Department of Electrical Engineering Physical Electronics, Tel Aviv University, Ramat Aviv 69978, Israel
[2] California Institute of Technology (Caltech), Pasadena, California 91125, USA

(Received 25 September 2019; revised manuscript received 2 December 2019; accepted 13 January 2020; published 13 February 2020)

Here we present a new paradigm of free-electron–bound-electron resonant interaction. This concept is based on a recent demonstration of the optical frequency modulation of the free-electron quantum electron wave function (QEW) by an ultrafast laser beam. We assert that pulses of such QEWs correlated in their modulation phase, interact resonantly with two-level systems, inducing resonant quantum transitions when the transition energy $\Delta E = \hbar\omega_{21}$ matches a harmonic of the modulation frequency $\omega_{21} = n\omega_b$. Employing this scheme for resonant cathodoluminescence and resonant EELS combines the atomic level spatial resolution of electron microscopy with the high spectral resolution of lasers.

DOI: 10.1103/PhysRevLett.124.064801

The reality of the quantum electron wave function and its interpretation have been a matter of debate since the inception of quantum theory [1,2]. Recent developments in ultrafast electron microscopy, and particularly photon-induced near-field electron microscopy (PINEM) [3–10] demonstrated the possibility of modulating the energy spectrum of single quantum electron wave packets (QEW) at discrete energy sidebands $\Delta E_n = n\hbar\omega_b$ by interaction with a laser beam of frequency ω_b. The interaction is made possible by a multiphoton emission or absorption process in the near field of a nanostructure [9,11], a foil [8,10], or a laser beat (pondermotive potential) [12,13]. It was also shown that due to the nonlinear energy dispersion of electrons in free space drift, the discrete energy modulation of the QEW turns into a tight bunching density modulation at attosecond short levels, corresponding to high spectral harmonics contents $\omega_n = n\omega_b$ in the expectation value of the QEW density $\langle|\Psi(r,t)|^2\rangle$. The physical reality of this sculpting of the QEW in the time and space (propagation coordinate, z) dimensions can be demonstrated in the interaction of such modulated QEWs with radiation [14,15]. Such bunching-phase-sensitive resonant stimulated radiative interactions (acceleration or deceleration) of QEW have been demonstrated recently experimentally with a second laser beam, phase-locked to the bunching frequency or its harmonic [10,12,16,17].

Here we propose a new concept of free-electron–bound-electron resonant interaction (FEBERI) based on the idea that optical frequency density modulated QEWs can interact resonantly with quantum electron transitions in matter at harmonics of its modulation frequency. Such interaction is shown schematically in Figs. 1(a) and 1(b) for the simple case of interaction with a single two-level system (2-LS) of a bound electron, e.g., in an atom, quantum-dot structure, defect center in crystal, etc. The interaction would lead to resonant transitions between the quantum levels 1 and 2 and corresponding energy loss or gain in the free electron energy. The resonant interaction can be monitored by measurement of the electron energy loss or gain spectrum (EELS, EEGS) [18], or by measuring the fluorescence due to excitation of the bound electron to the upper level 2 and its radiative relaxation to the lower level 1 or possible other levels. In this sense, the effect will be a resonant cathodoluminescence (RCL) effect, showing enhanced CL [19] emission of the sample when the harmonic frequency of the interacting QEW $n\omega_b$ matches the transition energy $n\hbar\omega_b \cong \Delta E = \hbar\omega_{1,2}$. Such a scheme can have a major impact on electron microscopy and material spectroscopy, combining the atomic level spatial resolution of electron microscope with the high spectral resolution of the laser. Such resolution can be instrumental also in quantum computing, addressing Q-bits based on 2-LS defect centers in crystals [20,21]. Furthermore, with intense localized pumping of atomic or nanometric 2-LS systems and microresonators, one may even consider development of microscopic single atom lasers [22].

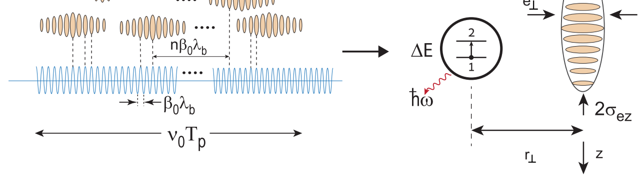

FIG. 1. A density-modulated quantum electron wave packet (a) passing near a two-level system (2LS) target (b), and exciting transitions and luminescence. (c) Enhanced excitation by a train of modulation-phase correlated QEWs.

A possible way of analyzing the proposed interaction scheme is by solving the Schrödinger equation for the scattering of an incident electron quantum wave packet by the electrons of an atomic system. This can be done numerically using a time dependent density functional theory (TDDFT) formulation based on the time dependent Kohn-Sham (TDKS) equations [23] (See Supplemental Material [24] SM-A). Taking an analytical approximation approach, the problem can be presented in terms of dipole coupling between the free QEW and the bound electron through their near-field induced electric fields. In this Letter we neglect the effect of the 2-LS dipole moment on the QEWs (neglecting their interaction quantum recoil), and assume that the bound electron transition is governed by the Schrödinger equation

$$i\hbar\frac{\partial}{\partial t}\Psi_b(\mathbf{r},t) = [H_0 + V^{wp}(\mathbf{r})]\Psi_b(\mathbf{r},t), \tag{1}$$

where $V^{wp} = -e\mathbf{E}(t)\cdot\mathbf{r}$, and $\mathbf{E}(t)$ is the field induced by the modulated QEW at the 2-LS location. For a single QEW, modulated at frequency ω_b and tightly bunched [9], we model its density as

$$n_e(\mathbf{r},t) = f_{e\perp}(\mathbf{r}_\perp)f_{et}(t-t_0-z/v)f_{\mathrm{mod}}(t-z/v_0), \tag{2}$$

where $f_{e\perp}(r_\perp)$ is a narrow normalized transverse distribution, $f_{et}(t) = \exp(-t^2/2\sigma_{et}^2)/\sqrt{2\pi}\sigma_{et}$, σ_{et} is the quantum wave packet duration, $f_{\mathrm{mod}}(t) = \sum_{n=-\infty}^{\infty} B_n e^{-in\omega_b t}$, and B_n are the coefficients of the harmonics. Maximal tight density bunching is attained after drift time $t_{D,\max} = T_b/(2\Delta p_m/p_0)$ past the laser modulation point, where $T_b = 2\pi/\omega_b$, and $\Delta p_m/p_0$ is the momentum modulation amplitude of the electron relative to the average momentum [9,15]. Substantially high amplitude ($B_n > 0.3$) harmonics are attainable up to the 20th harmonic [15] and beyond [25] (see Supplemental Material [24] SM-B).

The self-fields of the charge-modulated QEW are found from Maxwell equations similarly to the semiclassical calculation of EELS in electron microscopy [18]. For the assumption of a transverse distribution $f_{e\perp}(\mathbf{r}_\perp)$ narrow relative to the bunching wavelengths and an impact parameter $\mathbf{r}_\perp$ longer than the QEW width, but within the near field of the modulated QEW [see Figs. 1(a) and 1(b)]:

$$E(\mathbf{r},t) = \frac{e}{2\pi\epsilon_0}\frac{f_{et}(t-t_0-z/v)}{v^2\gamma_\epsilon\epsilon_r}\sum_n \omega_n B_n \mathbf{g}_n(\mathbf{r})e^{i\omega_n[t-(z/v)]}, \tag{3}$$

$$\mathbf{g}_n(\mathbf{r}_\perp) = \left[\frac{1}{\gamma_\epsilon}K_0\left(\frac{\omega_n r_\perp}{v\gamma_\epsilon}\right)\hat{\mathbf{z}} - K_1\left(\frac{\omega_n r_\perp}{v\gamma_\epsilon}\right)\hat{\mathbf{r}}_\perp\right], \tag{4}$$

with $\omega_n = n\omega_b$, $\gamma_\epsilon = 1/\sqrt{1-\epsilon_r\beta^2}$, $\epsilon_r = \epsilon/\epsilon_0$ $\beta = v/c$ $\mathbf{r} = (\mathbf{r}_\perp, z)$, $\mathbf{r}_\perp = (x,y)$ and K_m are modified Bessel functions. We then need to solve a simple 2-LS equation for the bound electron wave function $\Psi_b(\mathbf{r},t) = a_1(t)\varphi_1(\mathbf{r})e^{-iE_1t/\hbar} + a_2(t)\varphi_2(\mathbf{r})e^{-iE_2t/\hbar}$, where $\varphi_1(\mathbf{r})$, $\varphi_2(\mathbf{r})$ are the eigenvalues of the noninteracting 2-LS. This is a standard problem of coherent light interaction with quantum levels in matter [26,27], except that the field here is not a laser field, but the near field of the modulated QEW. It leads to the coupled-modes equations (see Supplemental Material [24] SM-C):

$$a_1'(t) = \frac{i}{\hbar}V_{21}^*(t)e^{i\omega_{21}t}a_2(t), \tag{5a}$$

$$a_2'(t) = \frac{i}{\hbar}V_{21}(t)e^{-i\omega_{21}t}a_1(t), \tag{5b}$$

where $\omega_{21} = (E_2 - E_1)/\hbar$, $V_{ij} = \int\varphi_i^*(\mathbf{r})V^{wp}(\mathbf{r},t)\varphi_j(\mathbf{r})d^3r$, and it is assumed that $V_{11} = 0$ $V_{22} = 0$ $V_{21} = V_{12}^*$.

We use the solution of these equations in two cases of interest: first, for a π-pulse half period Rabi oscillation case, in which the interaction Hamiltonian $V(t)$ and interaction time are large enough to produce complete transition of the bound electron from the ground to top level. Second, for the case of weak coupling, where we can only calculate the probability of exciting the upper level in one interaction event.

In the first case, we assume for simplicity a constant amplitude harmonic field $\mathbf{E}(t) = \mathbf{E}_0\cos(\omega_0 t - \varphi_0) = \frac{1}{2}\mathbf{E}_0 e^{i(\omega_0 t-\varphi_0)} + \mathrm{c.c.}$ and present the solution for the case of exact resonance, $\omega_0 = \omega_{1,2} = \Delta E/\hbar = (E_2 - E_1)/\hbar$, starting from the ground state $a_1(0) = 1$, $a_2(0) = 0$ (see solution for the general case in Refs. [26,27]). The occupation probabilities of the states are

$$P_2(t) = |a_2(t)|^2 = \sin^2(\Omega_R t/2),$$
$$P_1(t) = |a_1(t)|^2 = \cos^2(\Omega_R t/2), \tag{6}$$

where

$$\Omega_R = 2|V_{21}|/\hbar = \boldsymbol{\mu}_{21}\cdot\mathbf{E}_0/\hbar, \tag{7}$$

$\boldsymbol{\mu}_{21} = -e\mathbf{r}_{21}$ is the dipole moment of the 2-LS transition.

We now extend this model to the case of inducing a coherent 2-LS transition with a pulse of modulated QEWs [Eq. (2)]. Such an ensemble of QEWs may excite transitions in the 2-LS incoherently and randomly, with probability proportional to N_e. However, when the modulated envelopes of the QEWs are phase correlated, as shown in Fig. 1(c), the Rabi oscillation process will build up coherently throughout the entire pulse. The correlated optically modulated QEWs pulse density can be presented as a sum of individual QEW densities (2) arriving each at random time t_{0j} ($j = 1$ to N_e) at the 2-LS location

$$n_e(\mathbf{r},t) = f_{e\perp}(\mathbf{r}_\perp)f_{\mathrm{mod}}\left(t-\frac{z}{v}\right)\sum_1^{N_e} f_{et}\left(t-t_{0j}-\frac{z}{v}\right). \tag{8}$$

This scenario [Fig. 1(c)], is similar to the case of superradiance of a bunched electron beam. In this case the bunching of the electrons is modeled in terms of point particles [28] or quantum wave packets [15], and the bunched beam radiates at all harmonics $n\omega_b$ of the bunching frequency in proportion to N_e^2, similarly to Dicke's atomic superradiance [29,30].

In the present case, the nth harmonic component of the modulation-correlated electrons interacts coherently with a 2-LS. Consequently, when the modulation phases of the different QEWs are correlated [see Fig. 1(c)] (for example, if they were all *a priori* bunched by the same coherent laser beam), then the near fields of all wave packets, irrespective of their arrival times t_{oj}, add up coherently, but the sum of the QEW density distribution in Eq. (8) is replaced by the temporal distribution of the electron pulse (SM-D). Assuming for simplicity that the pulse envelope is uniform, of duration T_p, shorter than the relaxation or the decoherence time of the 2-LS, we replace $f_e(t)$ with $f_p(t) = 1/T_p$ in Eq. (3), and the relevant field component in Eq. (7) for the nth harmonic is

$$\mathbf{E_0} = \frac{1}{2\pi\epsilon_0}\frac{e\omega_n}{v^2\gamma_\epsilon\epsilon_r}\mathbf{g_n}(r_\perp)\frac{B_nN_e}{T_p}. \tag{9}$$

Interestingly enough the quantum features disappear in this case and the pulse duration T_p takes the role of the quantum wave packet size σ_{et}. It is noteworthy that the expressions for the density bunching amplitudes B_n have been derived independently for a pulse of laser-modulated particles beam in a point-particles model in connection to harmonic superradiance in FEL [28]. Here, following Ref. [9] we used a quantum wave packet model for the bunching, because the wave packet size $\sigma_{ez} = v_0\sigma_{et}$ is usually longer than an optical wavelength in a high quality TEM [14,31]. The consistency of the quantum and classical analyses of the bunching process in the case of multiple electrons is satisfying. Of course, the transition process in the 2-LS is by itself a quantum effect in any case.

Substituting Eq. (9) in Eq. (7), one can calculate, given the dipole moment μ_{12} and the electron number N_e in the pulse, the condition for complete population inversion:

$$\Omega_R T_p = \frac{2\alpha\omega_n}{c\beta^2\gamma_\epsilon\epsilon_r}\boldsymbol{\mu}_{\mathbf{21}}\cdot\mathbf{g_n}(r_\perp)B_nN_{e,\pi} = \pi, \tag{10}$$

with $\alpha = (1/4\pi\varepsilon_0)e^2/\hbar c = 1/137$ the fine-structure constant. Note that the pulse duration T_p cancelled out of condition (10), and it is insignificant, as long as it is shorter than the relaxation time of the upper level t_r. If this condition can be satisfied, it should be possible to obtain an efficient resonant CL (RCL) with a finite pulse of $N_{e,\pi}$ modulated QEWs interacting with a single 2-LS atom or a quantum dot or in bulk.

Another possible scenario is when $\Omega_R T_p \ll \pi$ (weak coupling). In this case, from Eq. (6),

$$P_2(T_p) \approx \left(\Omega_R\frac{T_p}{2}\right)^2 = \left(\frac{\alpha\omega_n}{c\beta^2\gamma_\epsilon\epsilon_r}\boldsymbol{\mu}_{\mathbf{21}}\cdot\mathbf{g_n}(r_\perp)B_nN_e\right)^2. \tag{11}$$

Noteworthy is the quadratic dependence on N_e of the transition probability of coherent resonant FEBERI and RCL as opposed to the linear dependence in conventional CL.

The coherent buildup of Rabi oscillation by a pulse of phase-correlated QEWs is demonstrated in Fig. 2(a), showing simulation (see Supplemental Material [24] SM-E) of population buildup of level 2 due to interaction with a pulse of N_e correlated QEWs having the same phase but arriving at random time t_{0j}. For comparison, simulation parameters are normalized to accumulate the same Rabi phase $\Phi_R(t) = \int_0^t \mu_{12}\bar{E}_0(t')dt'/\hbar$, on the average.

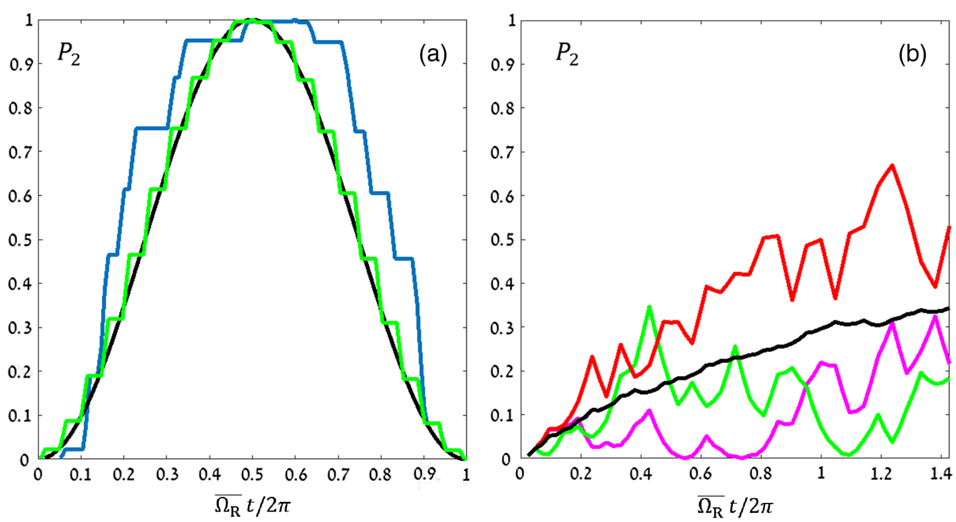

FIG. 2. Comparison of upper level population probability buildups by the field excitation of a pulse of modulated QEWs. (a) Excitation of Rabi oscillation with *correlated* wave packets: Green curve, QEWs arrive at equal time spacing; blue, at random time t_{0j}; black, a continuous modulated QEW. (b) Same, with *uncorrelated* modulated QEWs (φ_{0j} random); black is the average of events.

Therefore, their time is normalized to an effective Rabi frequency: $\bar{\Omega}_R = \Omega_R(N_e T_e/T_p)$. Figure 2(b) shows the buildup of the occupation probability of level 2 in the case of uncorrelated QEWs, namely, their phases $\varphi_{0j} = \omega_0 t_{0j}$ are random. Evidently the population growth P_2 is slower, and does not arrive to full occupation. The black curve is an average over several simulation events, confirming the initial linear buildup of the upper level population as a function of N_e in the absence of relaxation.

We now go back to present a general solution of Eq. (5B) in the limit of weak coupling, and apply it to compare the cases of a single finite size QEW, modulated QEWs, and the conventional point-particle limit. Whether a single QEW interaction with matter can be observed and measured is a fundamental physics question that has been considered in connection to interaction of QEW with light [15,32,33]; here we consider it in the case of interaction with matter.

The first-order solution of Eq. (5B) for a general finite time field pulse $\mathbf{E}(t)$ with perturbation Hamiltonian $V^{wp} = \boldsymbol{\mu}_{21} \cdot \mathbf{E}$, under the assumptions $a_1(t) \approx a_1(0) = 1$, $|a_2(t)| \ll 1$, is

$$a_2 = -\frac{i}{\hbar}\boldsymbol{\mu}_{21} \cdot \int_{-\infty}^{\infty} \mathbf{E}(t) e^{i\omega_{21}t} dt = -\frac{i}{\hbar}\boldsymbol{\mu}_{21} \cdot \breve{\mathbf{E}}(\omega_{21}), \quad (12)$$

where $\breve{\mathbf{E}}(\omega) = \mathcal{F}\{\mathbf{E}(t)\}$.

We first apply this expression for the case of an unmodulated QEW—Eq. (3) with $B_n = \delta_{n,0}$. The probability of exciting level 2 by N_e uncorrelated QEWs is

$$P_2^{\text{WP}} = N_e |a_2|^2 = N_e P_2^{\text{par}} |F_e(\omega_{21})|^2, \quad (13)$$

$$P_2^{\text{Part}} = \left(\frac{\alpha\omega_{21}}{c\beta^2\gamma_e\epsilon_r} \boldsymbol{\mu}_{\mathbf{21}} \cdot \mathbf{g_n}(r_\perp) \right)^2, \quad (14)$$

where for a Gaussian wave packet envelope $f_{et}(t) = (\sqrt{2\pi}\sigma_{et})^{-1} \exp(-t^2/2\sigma_{et}^2)$, one has $F_e(\omega) = \mathcal{F}\{f_{et}(t)\} = e^{-\omega^2\sigma_{et}^2/2}$. In the limit $\sigma_{et} \to 0$ of a point particle $P_2^{\text{WP}} \to P_2^{\text{Par}}$, as expected. On the other hand, for a long QEW $\omega_{21} \gg 1/\sigma_{et}$ the excitation probability decays. This is evidently a quantum effect, not predictable by a point-particle model of the electron. It is consistent with previous conjectures of decay of radiative interaction of a QEW in the limit $\omega\sigma_{et} = 2\pi\sigma_{ez}/\beta\lambda \gg 1$ with $\sigma_{ez} = v\sigma_{et}$, $\lambda = 2\pi c/\omega$, that are predicted in a semiclassical interaction model [14,15], but not verified in a QEW analysis of spontaneous emission by a single QEW [33].

In the interesting case of a modulated QEW, we insert in Eq. (13) the expression of the Fourier transform of Eq. (3) of a harmonic frequency n, such that $\omega_n \approx \omega_{21}$. For N_e uncorrelated modulated QEWs this results in

$$\begin{aligned} P_2^{M-\text{WP}} &= N_e |a_2|^2 = N_e P_2^{\text{par}} |B_n|^2 |F_e(\omega_{21})|^2 \\ &= N_e P_2^{\text{par}} |B_n|^2 e^{-(\omega_{21}-\omega_n)^2\sigma_{et}^2}. \end{aligned} \quad (15)$$

For very tight bunching it is possible to get high harmonic amplitudes up to about 20th harmonic [9] and higher [25], and attain resonant FEBERI transitions at frequencies $\omega_n = n\omega_b \gg \omega_b$ beyond the cutoff frequency of an unmodulated finite QEW $1/\sigma_{et}$. Comparison of Eqs. (15) to (13) (with $N_e = 1$) reveals the special characteristics of a modulated QEW of finite size.

The significant enhancement of FEBERI transition with a pulse of modulation correlated QEWs, as compared to conventional (point-particle) interaction, is evident when one compares Eq. (11) to Eqs. (14), (15) (for the case $N_{e,\pi} \gg N_e \gg 1$). In this case, the probability of excitation of the upper level by N_e modulated QEWs can be written as $P_2(T_p) = B_n^2 N_e^2 P_2^{\text{par}}$, namely, there is an enhancement factor $B_n^2 N_e$ relative to the excitation probability with N_e uncorrelated point-particle interaction events. This enhancement may amount to many orders of magnitude, and it would be also the enhancement ratio of resonant cathodoluminescence in a two-level system, whether the excited electrons relax radiatively to the ground level or to other quantum levels.

We can now estimate the viability of our new concepts of FEBERI and RCL, referring to real parameters of a material target of interest, such as NV defect centers in diamond. We first check how many phase-correlated modulated QEWs would be required to produce a full π-phase Rabi transition and satisfy Eq. (10). In diamond NV centers there is a 2-LS quantum transition of $\Delta E = 1.945$ eV [21], and it thus can be excited resonantly by the second harmonic field component of a pulse of QEWs, modulated by an infrared laser of $\lambda_b = 1.27$ μm. With a rough estimate $[g_n(r_\perp)B_n/\beta^2\gamma_\varepsilon\varepsilon_r] \approx 1$, one obtains $N_\pi = 2.2 \times 10^4$, which corresponds to 3.7×10^{-15} Coulomb. This may be excessive charge for the femtosecond laser driven photoemission techniques used in PINEM [9,34], and one may be concerned about energy spread and loss of modulation coherence due to Coulomb interaction scattering in the electron pulse [35]. However, since the relaxation time of the 2-LS can be quite long ($t_r = 13.5 \times 10^{-9}$ sec for a diamond NV center [21]), one may resort to distributing the charge over longer electron pulses or employing high rep-rate mode locked laser techniques [36], in order to mitigate the Coulomb scattering problem. Alternatively, if one operates in the weak coupling regime with a smaller number of correlated modulated QEWs (say, $N_e = 10^2 \langle\langle N_\pi)$, one can still attain an enhancement factor of RCL by a factor N_e relative to the conventional CL from the same number of electrons.

The new concepts of FEBERI and RCL with single QEWs and with an ensemble of correlated QEWs, were presented here in the framework of a simplified semiclassical model. They should lead to more elaborate theoretical formulation and experimental studies in both fundamental and applied physics research. The reality of the size and shape of a single electron wave function in its interaction with radiation has raised new interest in the old question of particle-wave duality [14,31–33,37]. The CL process provides an alternative way for probing the reality of the single electron wave function through interaction with a well defined 2-LS quantum transition. In this Letter we proposed that the interaction of a single electron with an atomic system in matter can depend, and thus be controlled, by the modulation of its quantum electron wave function by a coherent laser beam and by the history of its transport to the interaction point. In the case of interaction with single QEWs, this picture may be contrasted by an argument of collapse of the wave function to a point particle at the single interaction event [38]. In the case of an ensemble of identical correlated modulated QEWs, the wavepacket modulation resonant enhancement effect is well justified [39] and consistent with classical point-particle bunching analysis.

These ideas are expected to lead to a new way for studying fundamental questions of quantum theory. On the application side, the combination of these concepts with the atomic scale spatial resolution of electron microscopes can lead to development of a new kind of electron microscopy and spectroscopy on the level of single atom resolution. Besides diagnosis on the basis of the emitted radiation (RCL), the imprint of the resonant interaction on the free electrons spectrum can be revealed in a TEM instrument also through EELS measurement [resonant EELS (REELS)]. This, as well as other applications such as addressing individual 2-LS targets as Q bits (for example, diamond NV centers in quantum computer schemes [20]), resonant CL in bulk (rather than isolated atoms), quantum dots, etc, resonant directed superradiant emission in a grating configuration [40], and possibly localized lasing in microcavity lasers [22], are promising directions of further development of the new concepts presented here.

This Letter presented only the theoretical principles of a new interaction scheme. Their realization in the laboratory may require dedicated development of electron microscopy technology for improving the quality of the modulated QEW, controlling the electron emission from the cathode, mitigating the deleterious effect of Coulomb scattering [35], and improving the efficiency of QEW modulation by laser beam.

This research was supported in part by a grant from the Israel Science Foundation (ISF) and the German-Israeli Project Cooperation (DIP). We thank Tom Shalev and Bin Zhang for providing simulation results.

*Corresponding author.
gover@eng.tau.ac.il

[1] E. Schrödinger, An undulatory theory of the mechanics of atoms and molecules, Phys. Rev. **28**, 1049 (1926).
[2] M. Z. Born, Zur Quantenmechanik der Stoßvorgänge, Z. Phys. **37**, 863 (1926).
[3] B. Barwick, D. J. Flannigan, and A. H. Zewail, Photon-induced near-field electron microscopy, Nature (London) **462**, 902 (2009).
[4] F. J. García de Abajo, A. Asenjo-Garcia, and M. Kociak, Multiphoton absorption and emission by interaction of swift electrons with evanescent light fields, Nano Lett. **10**, 1859 (2010).
[5] S. T. Park, M. Lin, and A. H. Zewail, Photon-induced near-field electron microscopy (PINEM): Theoretical and experimental, New J. Phys. **12**, 123028 (2010).
[6] S. T. Park and A. H. Zewail, Relativistic effects in photon-induced near field electron microscopy, J. Phys. Chem. A **116**, 11128 (2012).
[7] K. E. Echternkamp, A. Feist, S. Schäfer, and C. Ropers, Ramsey-type phase control of free-electron beams, Nat. Phys. **12**, 1000 (2016).
[8] G. M. Vanacore, I. Madan, G. Berruto, K. Wang, E. Pomarico, R. J. Lamb, D. McGrouther, I. Kaminer, B. Barwick, F. J. G. de Abajo, and F. Carbone, Attosecond coherent control of free-electron wave functions using semi-infinite light fields, Nat. Commun. **9**, 2694 (2018).
[9] A. Feist, K. E. Echternkamp, J. Schauss, S. V. Yalunin, S. Schfer, and C. Ropers, Quantum coherent optical phase modulation in an ultrafast transmission electron microscope, Nature (London)**521**, 200 (2015).
[10] K. E. Priebe, C. Rathje, S. V. Yalunin, T. Hohage, A. Feist, S. Schäfer, and C. Ropers, Attosecond electron pulse trains and quantum state reconstruction in ultrafast transmission electron microscopy, Nat. Photonics **11**, 793 (2017).
[11] L. U. C. A. Piazza, T. T. A. Lummen, E. Quinonez, Y. Murooka, B. W. Reed, B. Barwick, and F. Carbone, Simultaneous observation of the quantization and the interference pattern of a plasmonic near-field, Nat. Commun. **6**, 6407 (2015).
[12] M. Kozák, N. Schönenberger, and P. Hommelhoff, Ponderomotive Generation and Detection of Attosecond Free-Electron Pulse Trains, Phys. Rev. Lett. **120**, 103203 (2018).
[13] M. Kozák, T. Eckstein, N. Schönenberger, and P. Hommelhoff, Inelastic ponderomotive scattering of electrons at a high-intensity optical travelling wave in vacuum, Nat. Phys. **14**, 121 (2018).
[14] A. Gover and Y. Pan, Dimension-dependent stimulated radiative interaction of a single electron quantum wavepacket, Phys. Lett. A **382**, 1550 (2018).
[15] Y. Pan and A. Gover, Spontaneous and stimulated radiative emission of modulated free-electron quantum wavepackets—semiclassical analysis, J. Phys. Commun. **2**, 115026 (2018).
[16] D. S. Black, U. Niedermayer, Y. Miao, Z. Zhao, O. Solgaard, R. L. Byer, and K. J. Leedle, Net Acceleration and Direct Measurement of Attosecond Electron Pulses in a Silicon Dielectric Laser Accelerator, Phys. Rev. Lett. **123**, 264802 (2019).
[17] N. Schönenberger, A. Mittelbach, P. Yousefi, U. Niedermayer, and P. Hommelhoff, Generation and Characterization of Attosecond Micro-Bunched Electron Pulse Trains via Dielectric Laser Acceleration, Phys. Rev. Lett. **123**, 264803 (2019).

[18] F. J. G. De Abajo, Optical excitations in electron microscopy, Rev. Mod. Phys. **82**, 209 (2010).
[19] M. Kociak and L. F. Zagonel, Cathodoluminescence in the scanning transmission electron microscope, Ultramicroscopy **176**, 112 (2017).
[20] J. R. Weber, W. F. Koehl, J. B. Varley, A. Janotti, B. B. Buckley, C. G. Van de Walle, and D. D. Awschalom, Quantum computing with defects, Proc. Natl. Acad. Sci. U.S.A. **107**, 8513 (2010).
[21] A. T. Collins, M. F. Thomaz, and B. J. Maria Isabel, Luminescence decay time of the 1.945 eV centre in type Ib diamond, J. Phys. C **16**, 2177 (1983).
[22] J. McKeever, A. Boca, A. D. Boozer, and J. Kimble, Experimental realization of a one-atom laser in the regime of strong coupling, Nature (London) **425**, 268 (2003).
[23] K. Tsubonoya, C. Hu, and K. Watanabe, Time-dependent density-functional theory simulation of electron wave-packet scattering with nanoflakes, Phys. Rev. B **90**, 035416 (2014).
[24] See Supplemental Material at http://link.aps.org/supplemental/10.1103/PhysRevLett.124.064801 for detailed derivation of the 2-LS transition rate and the simulation procedure.
[25] S. Nehemia, R. Dahan, M. Shentcis, O. Reinhardt, Y. Adiv, K. Wang, and I. Kaminer, Observation of the stimulated quantum Cherenkov effect, arXiv:1909.00757.
[26] M. Scully and S. Zubairy, *Quantum Optics* (Cambridge University Press, Cambridge, England, 1996).
[27] A. Yariv, *Optical Electronics*, 4th ed. (Oxford University Press, Oxford, 1995).
[28] A. Gover, R. Ianconescu, A. Friedman, C. Emma, N. Sudar, P. Musumeci, and C. Pellegrini, Superradiant and stimulated superradiant emission of bunched electron beams, Rev. Mod. Phys. **91**, 035003 (2019).
[29] R. H. Dicke, Coherence in spontaneous radiation processes, Phys. Rev. **93**, 99 (1954).
[30] A. Gover, Superradiant and stimulated-superradiant emission in prebunched electron-beam radiators. I. Formulation, Phys. Rev. ST Accel. Beams **8**, 030701 (2005).
[31] Y. Pan, B. Zhang, and A. Gover, Anomalous Photon-Induced Near-Field Electron Microscopy, Phys. Rev. Lett. **122**, 183204 (2019).
[32] J. P. Corson and J. Peatross, Quantum-electrodynamic treatment of photoemission by a single-electron wave packet, Phys. Rev. A **84**, 053832 (2011).
[33] Y. Pan and A. Gover, Spontaneous, and stimulated emissions of a preformed quantum free-electron wave function, Phys. Rev. A **99**, 052107 (2019).
[34] M. Kruger, M. Schenk, and P. Hommelhoff, Attosecond control of electrons emitted from nanoscale metal tip, Nature (London) **475**, 78 (2011).
[35] A. Feist, N. Bach, N. R. da Silva, T. Danz, M. Möller, K. E. Priebe, and S. Strauch, Ultrafast transmission electron microscopy using a laser-driven field emitter: Femtosecond resolution with a high coherence electron beam, Ultramicroscopy **176**, 63 (2017).
[36] L. Schares, R. Paschotta, L. Occhi, and G. Guekos, 40-GHz mode-locked fiber-ring laser using a Mach-Zehnder interferometer with integrated SOAs, J. Lightwave Technol. **22**, 859 (2004).
[37] R. Remez, A. Karnieli, S. Trajtenberg-Mills, N. Shapira, I. Kaminer, Y. Lereah, and A. Arie, Observing the Quantum Wave Nature of Free Electrons through Spontaneous Emission, Phys. Rev. Lett. **123**, 060401 (2019).
[38] N. J. Schilder, H. Agrawal, E. C. Garnett, and A. Polman, Phase-resolved surface plasmon scattering probed by cathodoluminescence holography, arXiv:1912.04240.
[39] http://www.feynmanlectures.caltech.edu/III_21.html.
[40] A. Halperin, A. Gover, and A. Yariv, Electron-beam-induced super-radiant emission from a grating, Phys. Rev. A **50**, 3316 (1994).